Vol. 66: 91–101, 2015
doi: 10.3354/cr01336

CLIMATE RESEARCH
Clim Res

Published October 6

Extreme rainfall and summer heat waves in Macau based on statistical theory of extreme values

Weiwen Wang[1,3], Wen Zhou[1,*], Soi Kun Fong[2], Ka Cheng Leong[2], Iu Man Tang[2], Sau Wa Chang[2], Weng Kun Leong[2]

[1]Guy Carpenter Asia-Pacific Climate Impact Centre, School of Energy and Environment, City University of Hong Kong, Hong Kong, PR China

[2]The Macao Meteorological and Geophysical Bureau, Macau, PR China

[3]*Present address:* School of Architecture, The Chinese University of Hong Kong, Hong Kong SAR, PR China

ABSTRACT: Macau has continuous meteorological observations for more than 100 yr, data which are rarely available in South China. This study first homogenizes long-term observations in Macau using procedures for change point detection and adjustment, and then applies the statistical theory of extreme values to investigate changes in meteorological extreme events, including extreme rainfall and summer heat waves, at this station. A Poisson-generalized Pareto (GP) model is applied to extreme rainfall modeling, while a statistical model established by extending the Poisson-GP method is applied to heat wave modeling. In this heat wave model, the frequency of summer heat waves is modeled by a Poisson distribution, their intensity is modeled by a GP distribution, and their duration is modeled by a geometric distribution. Results show that these statistical models permit realistic modeling of extreme events in Macau. Return levels of extreme rainfall and heat waves in Macau are estimated by the Poisson-GP model fitted to the daily rainfall amount and summer daily maximum temperatures, respectively. Trends of extreme events are introduced into these statistical models through changes in parameters. It is found that the frequency of extreme rainfall increases significantly in the observational record of Macau, while the positive trend in the intensity of extreme rainfall is nonsignificant. For changes in parameters in summer heat waves, a significant increasing trend in the frequency is found after an adjustment is applied to a detected change point in the temperature record, but the positive trends in the intensity and duration are nonsignificant.

KEY WORDS: Extreme rainfall · Heat wave · Theory of extreme values

1. INTRODUCTION

Extreme weather and climate events such as heat waves, cold surges, droughts, floods, and hurricanes (typhoons) have affected human society from its very beginning. Obtaining better understanding of the variation and underlying mechanisms of these meteorological extreme events in both past and present climate conditions is a key issue for prediction and risk assessment in the future (Easterling et al. 2000, Meehl et al. 2000). To achieve this, long-term observational records are needed. Macau has continuous meteorological observations going back >100 yr, data which are rarely available in China, particularly in South China (Wang et al. 1998, Ye et al. 1998, Qian & Zhu 2001). Changes in climate extreme events in China have been widely discussed (Qian & Lin 2004, Zhou et al. 2006, 2009, You et al. 2010, Qian et al.

*Corresponding author: wenzhou@cityu.edu.hk

2011, Li et al. 2012, Wang et al. 2013, 2014). However, previous studies may be based either on relatively short-term observations, say, a few decades, or on trends obtained from simple linear regression, which may not be suitable for obtaining changes in extreme events (Li et al. 2005, Nogaj et al. 2006, Brown et al. 2008, Wang et al. 2015). In the present study, we investigate changes in extreme rainfall and summer heat waves using long-term observations in Macau based on the statistical theory of extreme values.

There is a long tradition of using the statistical theory of extreme values in environmental applications. In early studies, the Generalized Extreme Value (GEV) distribution with unchanged parameters was applied in order to model simple climatic extreme events, usually in the form of block maxima, such as annual maxima of daily precipitation or temperature (e.g. Gumbel 1958). Such studies typically assumed stationarity, that is, an unchanging climate. Later, the Poisson-generalized Pareto (GP) model was used to describe all exceedances above a high threshold instead of just looking at block maxima (e.g. Todorovic & Zelenhasic 1970). More importantly, the theory has been extended to encompass temporal trends. The most common approach for dealing with nonstationarity is to allow for parametric changes with time in the distribution (e.g. Smith 1989). This approach jointly models the occurrence of an event (an exceedance of a high threshold) and its severity (the degree of excess over a high threshold). The exceedances are assumed to occur according to a Poisson distribution, while the excesses above the threshold are assumed to follow a GP distribution (e.g. Coles 2001).

One simplification in the Poisson-GP model is that it assumes independence of daily events. In fact, the probability of a wet (rainy) day being followed by another wet day is higher than being followed by a dry day in summer, and vice versa (Groisman et al. 1999). But for extreme rainfall, the probability of an extreme rainy day following another extreme rainy day is low; that is, the temporal dependence in the daily rainfall series at extreme levels is weak (e.g. Li et al. 2005). Therefore, the assumption of independence in the Poisson-GP model is reasonable in extreme rainfall modeling (Begueria et al. 2011). When it comes to extreme high temperatures, the probability of a hot day being followed by another hot day is high in summer. In the early studies of heat waves, it was common to decluster the data and model only frequency and severity (Zhang et al. 2004, Nogaj et al. 2006, Brown et al. 2008). In recent studies, an approach to modeling heat wave duration using the temporal dependence of excesses within a heat wave, rather than discarding these clusters, has been advocated (Furrer et al. 2010, Keellings & Waylen 2014). This approach is adopted in this study and applied to model heat waves in Macau. Here we use the term 'heat wave' to represent different durations of high temperature extremes, including a single hot day and hot spells with one or more consecutive hot days.

2. DATA AND METHODOLOGY

2.1. Data and homogenization

Focusing on extreme rainfall and summer heat waves in Macau, 2 meteorological parameters are used in the present study: daily rainfall and summer (June–August) daily maximum temperature (Tmax). Observational records of these parameters in Macau are available from the late 19th century but have many missing values in the early years. We select records from periods with credible quality data: rainfall data from 1907 and temperature from 1912. There are no missing values for daily rainfall and only one missing value, in June 1916, for summer daily Tmax in the selected records. The time series of daily rainfall in Macau from 1 Jan 1907 to 31 Dec 2013 is shown in Fig. 1a, while the time series of summer daily Tmax from 1912 to 2013 is shown in Fig. 1b.

The location of the Macau observation station changed twice after 1904. It was located at 113° 32′ 39′ E, 22° 11′ 45′ N (at an altitude of 65 m) from 1904 to May 1966, moved to 113° 32′ 32′ E, 22° 12′ 57′ N (57 m) in May 1966, and moved to 113° 34′ 08′ E, 22° 09′ 33′ N (110 m) in August 1996, where it has remained to the present. Based on the analysis of the difference in annual mean temperature between Macau and Hong Kong, Fong et al. (2010) suggested that there is no noticeable discontinuity in the observed temperature of Macau. In this study, the RHtestsV4 software package (Wang & Feng 2013) is used to detect, and adjust for, multiple change points that could exist in the observed series of Macau. This software package is based on the penalized maximal *t*-test and the penalized maximal *F*-test (Wang 2008a, 2008b). These tests are embedded in a recursive testing algorithm. The lag-1 autocorrelation (if any) of the time series is empirically taken into account. Homogeneity tests without reference series are applied to both monthly total rainfall and monthly means of daily

Tmax. This method is used because (1) no long-term (say, up to 100 yr) reference series is available. There were no observations in Hong Kong during World War II, and observations in nearby Zhuhai in mainland China started in 1962 (Qian et al. 2015), only a few years before the relocation of the Macau station in 1966. (2) As suggested by Wang & Feng (2013), in the analysis of the daily series, the functions in RHtestsV4 should be applied to the corresponding monthly series, and it is acceptable to apply the RHtestsV4 functions to the monthly total precipitation series.

When RHtestsV4 is applied, no change point is detected in the monthly total rainfall, and one change point in 1966 is detected in the temperature series (Fig. 1b). We deduce that the detected change point in temperature is artificial because observations in Macau were relocated in 1966, as mentioned above. The Quantile-Matching adjustment algorithm (Wang et al. 2010, Vincent et al. 2012) is used to adjust the daily Tmax in Macau. The adjusted series is shown in Fig. 1c. The following heat wave study is based on this adjusted data.

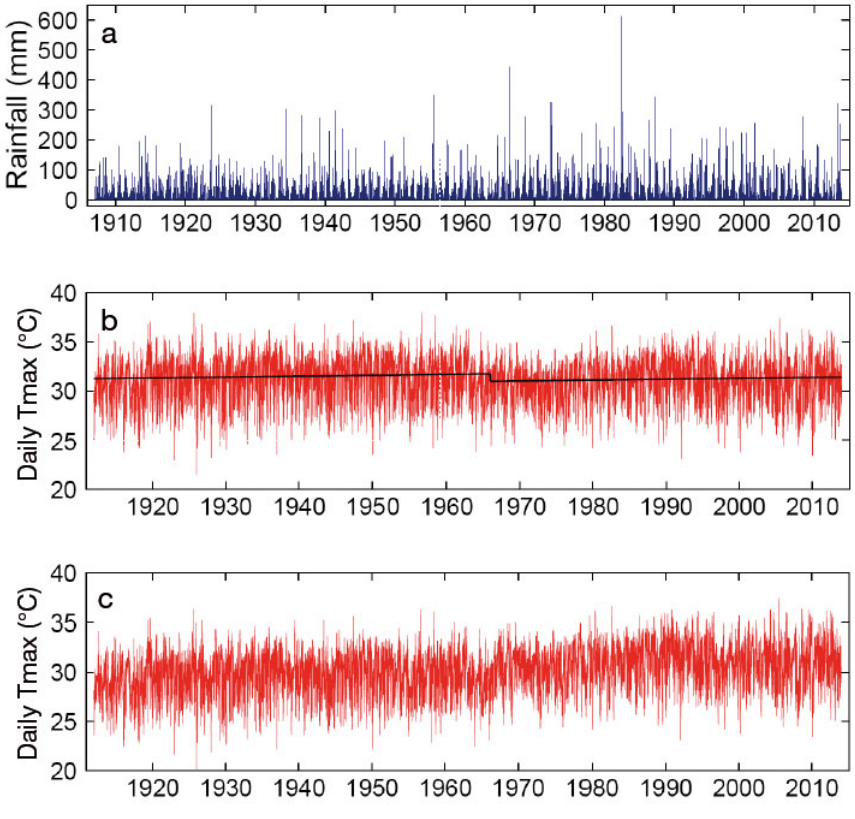

Fig. 1. Time series for Macau of (a) daily rainfall (mm) from 1 Jan 1907 to 31 Dec 2013; (b) summer (June–August) daily Tmax from 1912 to 2013, with a shift in the linear trend (black line) in 1966 detected by RHtestsV4; (c) the temperature time series adjusted using the Quantile-Matching algorithm

2.2. The Poisson-GP model for extreme rainfall

As introduced above, the Poisson-GP model is applied to extreme rainfall. Specifically, the annual frequency of extreme rainfall exceeding a high threshold is modeled by a Poisson distribution, and its intensity (the rainfall amount that is above the threshold for defining an extreme event) is modeled by a GP distribution. The probability mass function (PMF) of the Poisson distribution is given by:

$$P(k) = \frac{\lambda^k e^{-\lambda}}{k!}, \qquad k = 0,1,2, \tag{1}$$

where k is the number of events in a given year and λ is the Poisson parameter. A GP distribution is given by:

$$F(x;\xi,\sigma_u,u) = 1-\left[1+\xi\frac{x-u}{\sigma_u}\right]^{-\frac{1}{\xi}}, \; x>u, 1+\xi\frac{x-u}{\sigma_u}>0 \tag{2}$$

where x is the variable to be modelled, ξ stands for the shape parameter, and $\sigma_u > 0$ denotes the scale parameter depending on the selected threshold u. Parameter estimation in the Poisson-GP model is done using maximum likelihood methods.

The Poisson-GP model is further extended to allow for estimating trends in extreme rainfall frequency and intensity, and duration characteristics. One can consider parameters to be fixed within a given year but allow shifts from one year to another. That is, for each year x in the record period, $\lambda = \lambda(x)$ for the Poisson parameter, and $\sigma_u = \sigma_u(x)$ for the GP scale parameter. Since changes in the shape parameter of the GP distribution are rarely observed and difficult to model, this parameter is kept fixed. Trends are introduced through a generalized linear model (GLM) framework in the Poisson model and through covariate effects in the GP scale parameter.

Extreme events are easy to recognize but difficult to define, as the concept of 'extremeness' is strongly dependent on context (Diaz & Murnane 2008). To assess past changes in extreme events as well as possible future consequences, an adequate threshold for the definition of extreme events is important (Robinson 2001, Perkins & Alexander 2013). We have to choose a threshold that is sufficiently high, so that the GP distribution (Eq. 2) is essentially satisfied, but

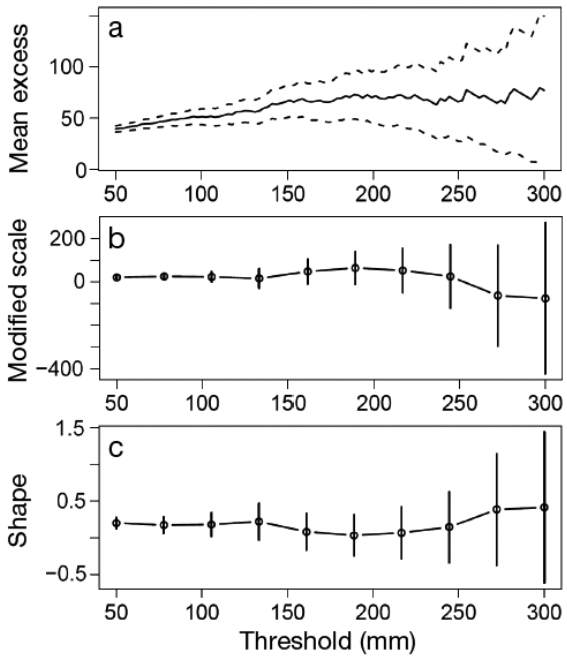

Fig. 2. (a) Mean residual life plot (dashed lines: confidence intervals), and (b) modified scale parameter σ_u and (c) shape parameter ξ estimates (error bars: confidence intervals) against threshold values for Macau daily rainfall

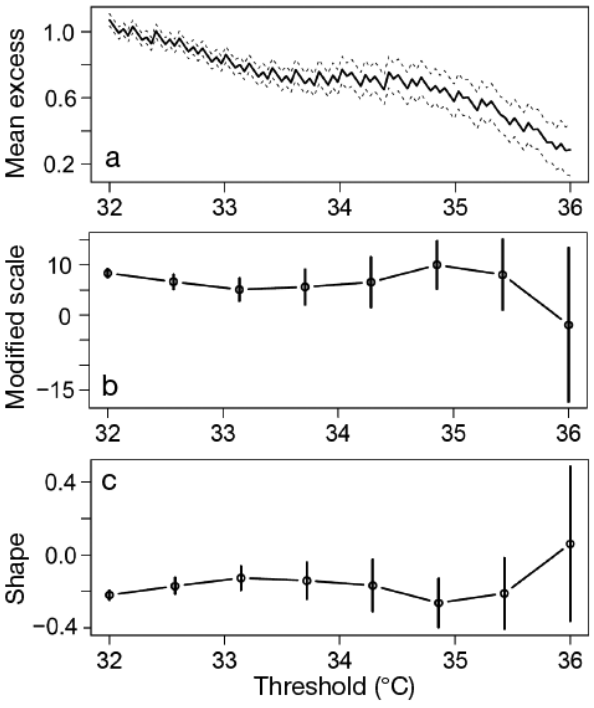

Fig. 3. (a) Mean residual life plot (dashed lines: confidence intervals), and (b) modified scale parameter σ_u and (c) shape parameter ξ estimates (error bars: confidence intervals) against threshold values for Macau daily Tmax

sufficiently low, so that there are enough excesses to estimate the parameters ξ and σ_u (Li et al. 2005). We adopt the criterion proposed by Coles (2001) for choosing the threshold, i.e. the use of 2 graphical tools: the mean residual life plot and the parameter stability plot. In practice, the scale parameter needs to be adjusted to remove the dependence on the threshold.

Fig. 2 shows the mean residual life plot and the parameter stability plot of Macau daily rainfall. We choose the threshold of $u = 100$ mm for extreme rainfall in Macau based on these plots. Fig. 2a is nearly linear, and both estimates σ_u and ξ are near constant for this u value. We further carry out a sensitivity analysis for this threshold selection. Diagnostic plots including a probability plot, quantile plot, and return level plot for GPD models fitted to daily rainfall data with various thresholds are generated (figures not shown), which allow the threshold selection to be revisited to see whether the asymptotic basis of the model is violated. Six thresholds (25, 50, 75, 100, 125 and 150 mm) are tested. It is found that a threshold of 50 mm or below is obviously too low, since the goodness-of-fit in the quantile plot is unconvincing, and the circles are located outside the confidence intervals on the return level plot. Basically, there is no noticeable change in results when thresholds higher than 75 mm are used. We therefore conclude that a threshold of 100 mm is a suitable choice.

2.3. Statistical modeling for heat waves

The statistical heat wave model extends the Poisson-GP method to model the frequency, duration, and intensity of heat waves. Specifically, the annual frequency of heat waves is modeled by a Poisson distribution, their intensity is modeled by a GP distribution, and their duration is modeled by a geometric distribution (Furrer et al. 2010, Wang et al. 2015). For temperature, negative shape parameters (ξ) of the GP distribution, that is, those with a bounded tail, are commonly obtained (e.g. Brown & Katz 1995). The probability mass function of the Poisson and GP distributions is given in Eqs. (1) & (2), respectively. A geometric distribution that can model the length (duration) of a heat wave is given by

$$P(k) = (1-\theta)^{k-1}\theta, \qquad k = 1, 2, \tag{3}$$

with the reciprocal of the parameter θ being the mean. Parameter estimation in the statistical heat wave model is done using maximum likelihood methods as well. Trends are introduced through a GLM framework in the geometric fitting. As in the Poisson-GP model introduced above, one can consider a parameter fixed over the summer season within a given year but allow shifts from one year to

another. That is, for each year x in the record period, $\theta = \theta(x)$ for the geometric parameter. See more details in Furrer et al. (2010).

The method of threshold selection for heat waves is the same as that for extreme rainfall. Fig. 3 shows the mean residual life plot and the parameter stability plot of Macau daily Tmax. A threshold of u = 34.0°C is chosen based on these graphical tools. In practice, the mean excess values and parameter estimates are computed from a relatively small quantity of data, so the plots will look only approximately linear or constant even when the GP distribution becomes valid. Confidence intervals are included to account for the effects of estimation uncertainty for our evaluation. But this still requires a good deal of subjective judgment. A sensitivity analysis similar to the case for extreme rainfall is conducted for this threshold selection (figures not shown). It is found that 33.0°C and below is too low for thresholds of the GPD models, while a threshold of 34.0°C is suggested to be a good choice.

3. CHANGES IN EXTREME RAINFALL

Having chosen the threshold u = 100 mm for extreme rainfall in Macau, for our rainfall data in 1907–2013 with n = 39 082 daily observations, we get N_u = 251 excesses. The number of rainy days among these 107 yr is 13406 (not including trace rain <0.2 mm). The number of days with extreme rainfall accounts for about 1.9% of the total rainy days. Fig. 4 shows the fitting of extreme rainfall by the Poisson-GP model in Macau, suggesting that this approach can realistically model the mean (i.e. stationary) intensity and frequency of extreme rainfall. Observations are shown in bars (Fig. 4a for intensity) and circles (Fig. 4b for frequency), while fittings of the statistical model are shown in red lines. For the frequency of extreme rainfall, observations in Fig. 4b give an occurrence of 1 to 3 d yr^{-1} with a maximum probability, and a maximum occurrence of 9 d in one year during these 107 yr. Meanwhile, threshold and fitting parameters (±SE) are given in Table 1. The GP scale parameter (σ_u) and shape parameter (ξ) for Macau extreme rainfall are 43.71 and 0.15, respectively. The Poisson parameter (λ) is 2.35. Actually, λ is the mean frequency of the fitted extreme event; that is, the mean of extreme rainy days in Macau is 2.35 d yr^{-1} as estimated by the Poisson-GP model.

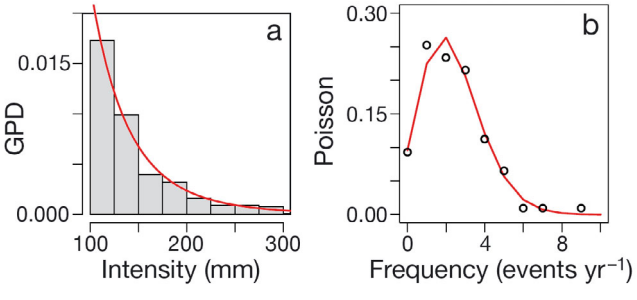

Fig. 4. Observed values for (a) intensity (mm d^{-1} above the defined threshold) and (b) frequency (events yr^{-1}) of extreme rainfall in Macau fitted to the generalized Pareto (GPD) and Poisson distributions, respectively (red lines)

Table 1. Thresholds and fitting parameters (standard errors in parentheses) of extreme rainfall and summer heat waves in Macau. The GP, Poisson, and geometric model is for fitting intensity, frequency, and duration of extreme events, respectively

Parameters	Extreme rainfall	Heat wave
Threshold (u)	100.0 mm	34.0°C
GP scale (σ_u)	43.71 ± 4.192	1.04 ± 0.092
GP shape (ξ)	0.15 ± 0.073	−0.23 ± 0.059
Poisson (λ) (events yr^{-1})	2.35 ± 0.290	2.39 ± 0.300
Geometric (θ) (d^{-1})	—	0.60 ± 0.037

It is usually more convenient to interpret the extreme value model in terms of quantiles or return levels, rather than in terms of individual parameter values (Coles 2001). To further characterize extreme rainfall in Macau, we estimate the return levels by the Poisson-GP model fitted to daily rainfall data. The result is shown by the solid red line of Fig. 5. The 95% confidence intervals of these estimations are

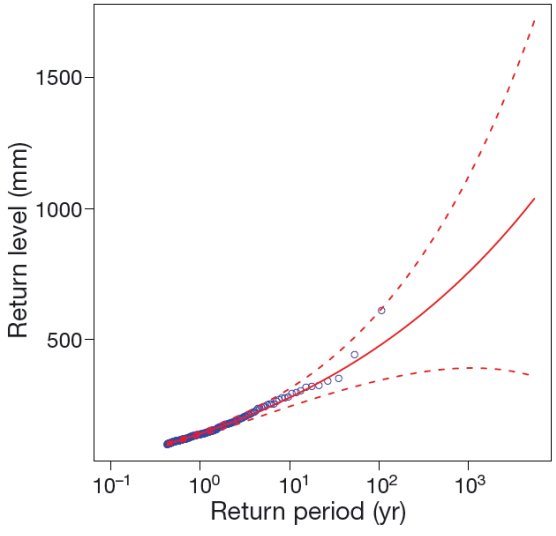

Fig. 5. Return level plot for threshold excess model fitted to daily rainfall data in Macau during 1907–2013 (solid line; dashed lines denote the 95% confidence interval), and observations for these 107 years (blue circles)

Table 2. Mean return levels (95% confidence intervals in parentheses) estimated using a threshold excess model fitted to daily rainfall data in Macau

Return period (yr)	Return level (mm)
5.5	236.4 (213.4, 259.5)
10.9	283.7 (247.6, 319.8)
54.7	415.8 (320.1, 511.5)
109.1	483.3 (345.9, 620.7)
217.6	558.5 (367.1, 749.8)

shown by red dashed lines and the observations are shown by blue circles. For quantitative description, it is more convenient to give return levels on an annual scale, that is, the N-yr return level is the level expected to be exceeded once every N yr. The return levels (with the 95% confidence intervals) of extreme rainfall in Macau corresponding to some typical return periods, e.g. approximately 5, 10, 50, 100, and 200 yr, are listed in Table 2. For example, the return level of a given 54.7-yr return period is estimated at 415.8 mm (95% confidence interval: 320.1 to 511.5 mm).

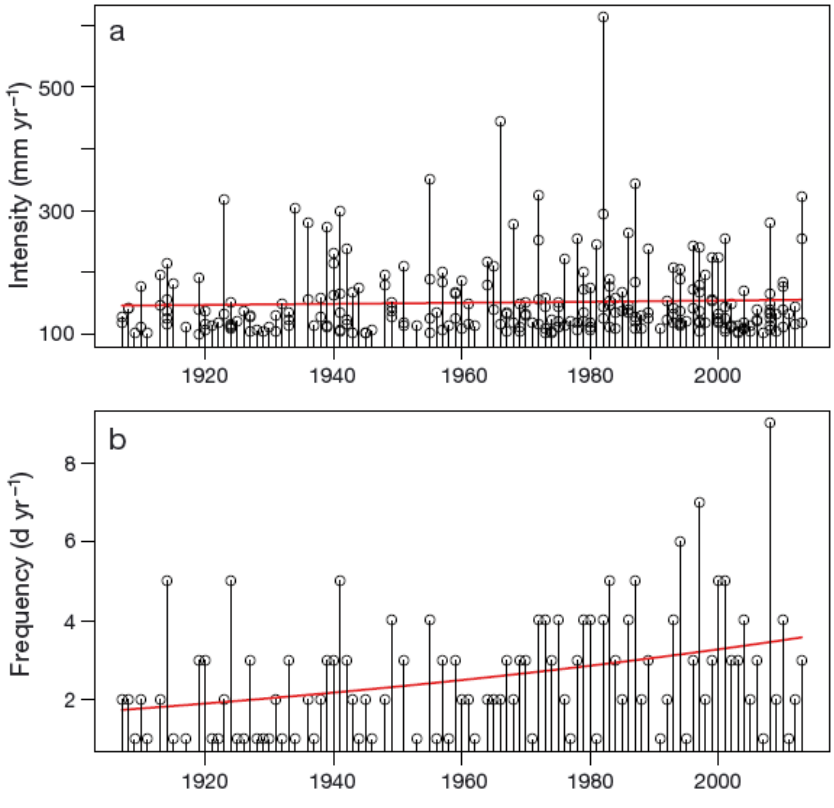

Fig. 6. Trends (red lines) of (a) intensity (above the defined threshold) and (b) frequency of extreme rainfall in Macau during 1907–2013 estimated by the GP and Poisson distributions, respectively. The stems represent observed values

Table 3. Nonstationary parametric trends (p-values in parentheses) in a Poisson-generalized Pareto (GP) model for extreme rainfall and statistical heat wave model in Macau

Trend	Extreme rainfall	Heat wave
GP scale (σ_u)	0.002 (0.5)	0.002 (0.150)
Poisson (λ)	0.007 (0.001)	0.006 (0.011)
Geometric (θ)	—	0.004 (0.337)

The last step is to obtain parametric trends of the extreme rainfall from the Poisson-GP model through the GLM framework (for the Poisson distribution) and covariate effects (for the GP distribution), as introduced in the methodology. The results are shown in Fig. 6, where the stems represent the observed year-to-year variations of extreme rainfall intensity (Fig. 6a) and frequency (Fig. 6b) in Macau during 1907–2013. When nonstationarity is introduced into the model, parametric trends of extreme rainfall are obtained. The red lines in Fig. 6 show the parametric trends of extreme rainfall components (intensity and frequency). The trends are 0.002 and 0.007 yr^{-1} for intensity and frequency, respectively (Table 3). p-values of the log-likelihood test estimated in the Poisson-GP model suggest that the trend of intensity is nonsignificant, while the trend of frequency is significant at the 0.01 level (p-values <0.01).

We further demonstrate how the statistical model estimates trends in extreme events by taking the frequency of extreme rainfall in Macau (Fig. 6b) as an example. The trend in the number of extreme rainy days is estimated based on a fitted nonstationary Poisson distribution where the parameter rate changes with the year (x): $\lambda(x) = \exp(\beta_0 + \beta_1 x)$. The GLM framework is used to estimate the parameters. Specifically, for the number of extreme rainy days in Macau, the trend is estimated by $\exp(-12.34 + 0.007x)$. It represents a proportionate increase of exp (0.007) in extreme rainy days, which is significant at the 0.01 level (Table 3), while −12.34 stands for the intercept. Simple linear regression to estimate the trend in the number of extreme rainy days is not recommended for 2 reasons: (1) the trend estimation based on the linear

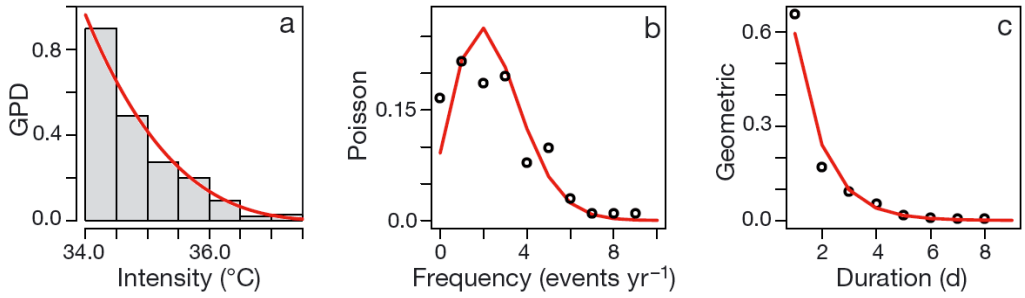

Fig. 7. Observed values for (a) intensity (°C above the defined threshold), (b) frequency and (c) duration of heat waves in Macau fitted to the generalized Pareto (GP), Poisson and geometric distributions, respectively (red lines)

model assumes the data follow a normal (Gaussian) distribution, which is not realistic for modeling extreme events; (2) the linear trend fails to capture the nonlinear behavior in the number of extreme rainy days. For the example of extreme rainfall frequency in Macau, the linear trend can be estimated by $-31.18 + 0.017x$, with a slope of 0.017 d yr^{-1} (intercept of −31.18), which indeed fails to capture the nonlinear trend in the number of extreme rainy days. This illustrates the key advantage of trend estimation in extreme meteorological events based on the statistical theory of extreme values.

4. CHANGES IN SUMMER HEAT WAVES

Fig. 7 shows how realistic the statistical model is in fitting the mean (stationary) intensity, frequency, and duration of heat waves in Macau. Observations are shown in bars (Fig. 7a for intensity) and circles (Fig. 7b for frequency and Fig. 7c for duration), while fittings of the statistical model are shown in red lines. Threshold and fitting parameters (±SE) are given in Table 1. The GP scale parameter (σ_u) and shape parameter (ξ) for Macau heat waves are 1.04 and −0.23, respectively. The Poisson parameter (λ) is 2.39, implying that the mean frequency of heat waves in Macau is estimated at 2.39 events yr^{-1}. The geometric distribution parameter (θ) is 0.60, implying a mean heat wave duration of 1.67 d (θ^{-1}) in Macau. In addition, observations in Fig. 7b give an occurrence of 1 to 3 events yr^{-1} with a maximum probability, and a maximum occurrence of 9 events in one year in 1912–2013. Observations in Fig. 7c show that a duration of 1 d has a maximum probability, and the longest duration can be up to 8 d in these 102 yr.

Return levels for the threshold excess model fitted to daily Tmax in Macau are estimated and shown in Fig. 8. Quantitative examples corresponding to 5 typical return periods are listed in Table 4. For instance,

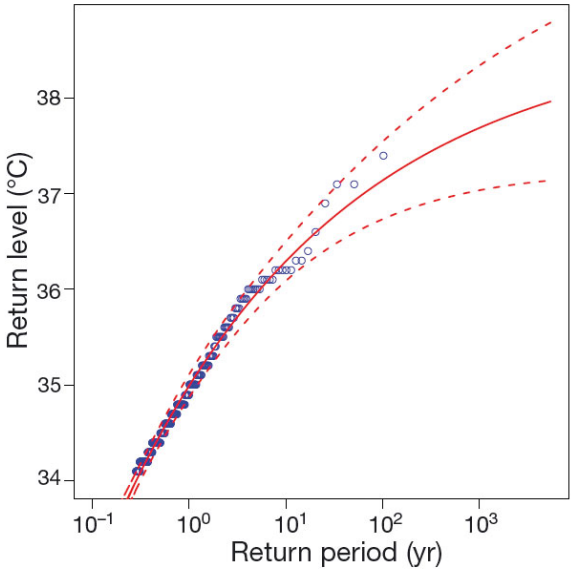

Fig. 8. Return level plot for threshold excess model fitted to daily Tmax in Macau during 1912–2013 (solid line; dashed lines denote the 95% confidence interval), and observations for these 102 years (blue circles)

the return level corresponding to a 10.9 yr return period is estimated at 36.3°C (95% confidence interval: 36.1 to 36.5°C); the return level corresponding to a 108.7-yr return period is estimated at 37.2°C (95% confidence interval: 36.7 to 37.6°C). We suggest that

Table 4. Mean (95% confidence intervals in parentheses) return levels estimated using a threshold excess model fitted to daily Tmax in Macau

Return period (yr)	Return level (°C)
5.4	36.0 (35.8, 36.2)
10.9	36.3 (36.1, 36.5)
54.5	36.9 (36.6, 37.3)
108.7	37.2 (36.7, 37.6)
216.9	37.3 (36.9, 37.8)

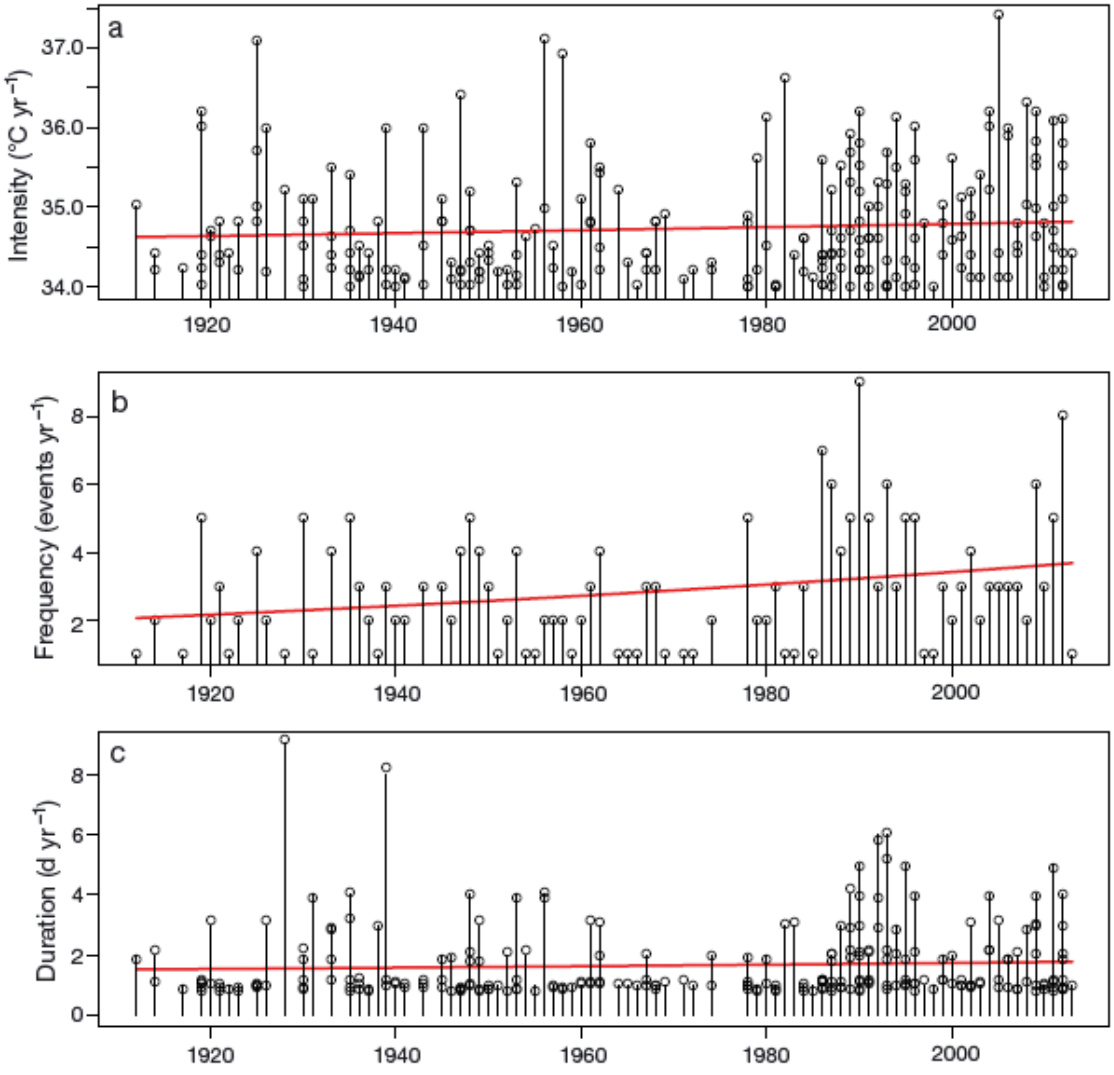

Fig. 9. Trends (red lines) of (a) intensity (above the defined threshold), (b), frequency and (c) duration of heat waves in Macau during 1912–2013 estimated by the GP, Poisson, and geometric distributions, respectively. The stems represent the observed values

these estimations of return levels using the threshold excess model can be helpful for social applications, such as risk assessment.

Finally, nonstationary parametric trends of heat wave intensity, frequency, and duration in Macau during 1912–2013, estimated by the GP, Poisson, and geometric distributions, are shown in the red lines of Fig. 9. The trends are 0.002, 0.006, and 0.004 yr^{-1} for heat wave intensity, frequency, and duration, respectively (Table 3). The p-values of the log-likelihood test estimated by the statistical heat wave model are shown in Table 3, which demonstrates that the increasing trend of heat wave frequency is significant at the 0.05 level, while the increasing trends of heat wave intensity and duration with large p-values are nonsignificant.

5. DISCUSSION AND CONCLUSIONS

Meteorological observations in China started mainly in the 1950s or 1960s (e.g. Li & Yan 2009). The present study investigates changes in extreme rainfall and summer heat waves using the theory of extreme values based on more than 100 yr of observations in Macau. Results show that the stationary Poisson-GP model can fit the frequency and intensity of extreme rainfall realistically (Fig. 4), while the statistical heat wave model with a geometric distribution added to the Poisson-GP model can simulate the intensity, frequency, and duration of heat waves (Fig. 7). Return levels of 2 climate extremes in Macau are estimated by the Poisson-GP model fitted to the daily rainfall amount and summer daily Tmax (Figs. 5

& 8), as these quantities are more convenient for interpreting the extreme value model than parameter values. Furthermore, return levels estimated by the threshold excess model can be helpful for social applications, such as risk assessment.

When it comes to time-dependent trends, ordinary parametric trend estimation (i.e. least squares regression) is not recommended, mainly because it requires the residual time series to be normally distributed, which is likely to be violated for time series of extreme events. Hence, nonparametric methods for trend detection, which require only that the data be independent, are widely used (Kunkel et al. 1999, Alexander et al. 2006, Haylock et al. 2006, New et al. 2006, Alexander & Arblaster 2009, Birsan et al. 2014, Deng et al. 2014, Pingale et al. 2014). The nonparametric Mann-Kendall test (Mann 1945, Kendall 1975) and the Kendall's tau-based slope estimator (Sen 1968, Wang & Swail 2001) are most frequently utilized in these studies. The former tests the direction (increase or decrease) and the significance of the trend, while the latter quantifies the magnitude of this trend (e.g. Chu et al. 2014). To complement these nonparametric methods, nonstationary GEV approaches are incorporated in some studies (Westra et al. 2013, Chen & Chu 2014, Bennett et al. 2015). However, if the distributional form is known, a parametric method usually has a better test power (Zhai et al. 2005). Zhang et al. (2004) compared the least squares method, the Kendall's tau-based method, and the GEV method and concluded that ordinary least squares regression is the least reliable, the Kendall's tau-based method provides some improvement, and explicit consideration of the extreme value distribution when computing the trend always outperforms these 2 methods. In a recent review of trend analysis, Madsen et al. (2014) also suggested that parametric tests seem to be the most powerful for extreme value data when the distributional assumptions (e.g. GEV or GP distribution) are fulfilled. We therefore suggest that trends of extreme events be introduced to parametric changes in fittings of extreme values through a GLM framework and covariate effects. The results show that the frequency of both extreme rainfall and summer heat waves increases significantly, while the trends of the intensity of extreme rainfall, and the intensity and duration of summer heat waves, are all positive but nonsignificant (Table 3).

The increasing trends of climate extremes detected in this study are noteworthy. Changes in extreme precipitation in South China or the Pearl River Basin have been investigated (e.g. Ning & Qian 2009, Zhang et al. 2009, Gemmer et al. 2011). Nevertheless, all of these previous studies utilized data only from recent decades, after the 1950s or 1960s, when meteorological observations were widely available in the region. Furthermore, it has been pointed out that, in the context of global warming, increasing temperature trends in Macau are weaker compared to other adjacent regions in the Pearl River Delta, such as Hong Kong and Guangzhou, particularly in the boreal summer (Fong et al. 2010). It is also found that the warming in Macau occurs mainly in minimum temperature rather than Tmax (Xu et al. 2007). In this study we reveal that the frequency of summer heat waves in Macau increases significantly in terms of nonstationary parametric trends in the statistical model during 1912–2013. This significant increase in heat wave frequency is, to some extent, a consequence of the adjustment in the temperature record (Fig. 1c). If the statistical heat wave model is implemented in the original time series of daily Tmax given in Fig. 1b (results not shown), it is found that increasing trends of heat waves are nonsignificant, i.e. all 3 p-values of the log-likelihood test estimated in the heat wave model are larger than the commonly used significance levels of 0.01 or 0.05. However, we can deduce that the detected change point in 1966 is artificial, as it is not only significant in the detection but also matches the year the weather station was relocated. Therefore, homogenization is required, and it demonstrates that the increasing trend in the frequency of summer heat waves in Macau is significant.

Finally, the area around the Pearl River Delta has undergone rapid urbanization. This implies that anthropogenic warming induced by urbanization and changes in land use may have contributed a portion of the warming (e.g. Jones et al. 2008, Hu et al. 2010). Identification of natural and anthropogenic forcing for the increasing extreme temperature as well as extreme rainfall in the region is needed in further studies. Extreme value analysis that incorporates atmospheric patterns in the distribution parameter estimates can be used to assess the dependence of extreme events on atmospheric forcing (Photiadou et al. 2014). But for dynamical analysis of more than 100 yr, the shortage of simultaneous long-term large-scale atmospheric data is a limitation.

Acknowledgements. This study is supported by the Macao Meteorological and Geophysical Bureau (SMG) Project 9231048, National Nature Science Foundation of China Grants 41175079 and 41375096, and the CityU Strategic Research Grant 7004164. We thank Dr. Yun Li for suggestions on the statistical theory of extreme values. We are grateful to the anonymous reviewers for their constructive comments.

LITERATURE CITED

Alexander LV, Arblaster JM (2009) Assessing trends in observed and modelled climate extremes over Australia in relation to future projections. Int J Climatol 29: 417–435

Alexander LV, Zhang X, Peterson TC and others (2006) Global observed changes in daily climate extremes of temperature and precipitation. J Geophys Res 111: D05109, doi:10.1029/2005JD006290

Begueria S, Angulo-Martinez M, Vicente-Serrano SM, López-Moreno JI, El-Kenawy A (2011) Assessing trends in extreme precipitation events intensity and magnitude using non-stationary peaks-over-threshold analysis: a case study in northeast Spain from 1930 to 2006. Int J Climatol 31:2102–2114

Bennett KE, Cannon AJ, Hinzman L (2015) Historical trends and extremes in boreal Alaska river basins. J Hydrol (Amst) 527:590–607

Birsan MV, Dumitrescu A, Micu DM, Cheval S (2014) Changes in annual temperature extremes in the Carpathians since AD 1961. Nat Hazards 74:1899–1910

Brown BG, Katz RW (1995) Regional analysis of temperature extremes: spatial analog for climate change? J Clim 8: 108–119

Brown SJ, Caesar J, Ferro CAT (2008) Global changes in extreme daily temperature since 1950. J Geophys Res Atmos 113:D05115, doi:10.1029/2006JD008091

Chen YR, Chu PS (2014) Trends in precipitation extremes and return levels in the Hawaiian Islands under a changing climate. Int J Climatol 34:3913–3925

Chu PS, Chen DJ, Lin PL (2014) Trends in precipitation extremes during the typhoon season in Taiwan over the last 60 years. Atmos Sci Lett 15:37–43

Coles S (2001) An introduction to statistical modeling of extreme values. Springer, London

Deng H, Chen Y, Shi X, Lia W, Wanga H, Zhanga S, Fanga G (2014) Dynamics of temperature and precipitation extremes and their spatial variation in the arid region of northwest China. Atmos Res 138:346–355

Diaz HF, Murnane RJ (2008) Climate extremes and society. Cambridge University Press, Cambridge

Easterling DR, Meehl GA, Parmesan C, Changnon SA, Karl TR, Mearns LO (2000) Climate extremes: observations, modeling, and impacts. Science 289:2068–2074

Fong S, Wu C, Wang A, He X and others (2010) Analysis of surface air temperature change in Macao during 1901–2007. Adv Clim Change Res 1:84–90

Furrer EM, Katz RW, Walter MD, Furrer R (2010) Statistical modeling of hot spells and heat waves. Clim Res 43: 191–205

Gemmer M, Fischer T, Jiang T, Su B, Liu LL (2011) Trends in precipitation extremes in the Zhujiang River Basin, South China. J Clim 24:750–761

Groisman PY, Karl TR, Easterling DR, Knight RW, and others (1999) Changes in the probability of heavy precipitation: important indicators of climatic change. Clim Change 42: 243–283

Gumbel EJ (1958) Statistics of extremes. Columbia University Press, New York, NY

Haylock MR, Peterson TC, Alves LM, Ambrizzi T and others (2006) Trends in total and extreme South American rainfall in 1960–2000 and links with sea surface temperature. J Clim 19:1490–1512

Hu Y, Dong W, He Y (2010) Impact of land surface forcings on mean and extreme temperature in eastern China. J Geophys Res 115:D19117. doi:10.1029/2009JD013368

Jones PD, Lister DH, Li Q (2008) Urbanization effects in large-scale temperature records, with an emphasis on China. J Geophys Res 113:D16122, doi:10.1029/2008JD009916

Keellings D, Waylen P (2014) Increased risk of heat waves in Florida: characterizing changes in bivariate heat wave risk using extreme value analysis. Appl Geogr 46:90–97

Kendall MG (1975) Rank correlation methods. Griffin, London

Kunkel KE, Andsager K, Easterling DR (1999) Long-term trends in extreme precipitation events over the conterminous United States and Canada. J Clim 12:2515–2527

Li Z, Yan ZW (2009) Homogenized daily mean/maximum/minimum temperature series for China from 1960–2008. Atmos Oceanic Sci Lett 2:237–243

Li Y, Cai W, Campbell EP (2005) Statistical modeling of extreme rainfall in southwest Western Australia. J Clim 18:852–863

Li XZ, Wen ZP, Zhou W, Wang DX (2012) Atmospheric water vapor transport associated with two decadal rainfall shifts over East China. J Meteorol Soc Jpn 90:587–602

Madsen H, Lawrence D, Lang M, Martinkovad M, Kjeldsene TR (2014) Review of trend analysis and climate change projections of extreme precipitation and floods in Europe. J Hydrol (Amst) 519:3634–3650

Mann HB (1945) Nonparametric trends against test. Econometrica 13:245–259

Meehl GA, Karl T, Easterling DR, Changnon S (2000) An introduction to trends in extreme weather and climate events: observations, socioeconomic impacts, terrestrial ecological impacts, and model projections. Bull Am Meteorol Soc 81:413–416

New M, Hewitson B, Stephenson DB, Tsiga A and others (2006) Evidence of trends in daily climate extremes over southern and west Africa. J Geophys Res 111:D14102, doi:10.1029/2005JD006289

Ning L, Qian YF (2009) Interdecadal change in extreme precipitation over South China and its mechanism. Adv Atmos Sci 26:109–118

Nogaj M, Yiou P, Parey S, Malek F, Naveau P (2006) Amplitude and frequency of temperature extremes over the North Atlantic region. Geophys Res Lett 33:L10801, doi:10.1029/2005GL024251

Perkins SE, Alexander LV (2013) On the measurement of heat waves. J Clim 26:4500–4517

Photiadou C, Jones MR, Keellings D, Dewes CF (2014) Modeling European hot spells using extreme value analysis. Clim Res 58:193–207

Pingale SM, Khare D, Jat MK, Admowski J (2014) Spatial and temporal trends of mean and extreme rainfall and temperature for the 33 urban centers of the arid and semi-arid state of Rajasthan, India. Atmos Res 138:73–90

Qian W, Lin X (2004) Regional trends in recent temperature indices in China. Clim Res 27:119–134

Qian W, Zhu Y (2001) Climate change in China from 1880–1998 and its impact on the environmental condition. Clim Change 50:419–444

Qian C, Yan ZW, Wu Z, Fu CB, Tu K (2011) Trends in temperature extremes in association with weather-intraseasonal fluctuations in eastern China. Adv Atmos Sci 28:297–309

Qian C, Zhou W, Fong SK, Leong KC (2015) Two approaches for statistical prediction of non-Gaussian climate extre-

mes: a case study of Macao hot extremes during 1912–2012. J Clim 28:623–636
Robinson PJ (2001) On the definition of a heat wave. J Appl Meteorol 40:762–775
Sen PK (1968) Estimates of the regression coefficient based on Kendall's tau. J Am Stat Assoc 63:1379–1389
Smith RL (1989) Extreme value analysis of environmental time series: an application to trend detection in ground-level ozone (with discussion). Stat Sci 4:367–393
Todorovic P, Zelenhasic E (1970) A stochastic model for flood analysis. Water Resour Res 6:1641–1648
Vincent LA, Wang XL, Milewska EJ, Wan H, Feng Y, Swail V (2012) A second generation of homogenized Canadian monthly surface air temperature for climate trend analysis. J Geophys Res Atmos 117:D18110, doi:10.1029/2012JD017859
Wang XL (2008a) Accounting for autocorrelation in detecting mean shifts in climate data series using the penalized maximal *t* or *F* test. J Appl Meteorol Climatol 47:2423–2444
Wang XL (2008b) Penalized maximal *F* test for detecting undocumented mean shift without trend change. J Atmos Ocean Technol 25:368–384
Wang XL, Feng Y (2013) RHtestsV4 user manual. Climate Research Division, Environment Canada, Ontario. http://etccdi.pacificclimate.org/software.shtml
Wang XL, Swail VR (2001) Changes in extreme wave heights in Northern Hemisphere oceans and related atmospheric circulation regimes. J Clim 14:2204–2221
Wang S, Ye J, Gong D, Zhu J (1998) Construction of mean annual temperature series for the last one hundred years in China. Quart J Appl Meteorol 9:392–401 (In Chinese)
Wang XL, Chen H, Wu Y, Feng Y, Pu Q (2010) New techniques for the detection and adjustment of shifts in daily precipitation data series. J Appl Meteorol Climatol 49:2416–2436
Wang W, Zhou W, Wang X, Fong SK, Leong KC (2013) Summer high temperature extremes in Southeast China associated with the East Asian jet stream and circumglobal teleconnection. J Geophys Res Atmos 118:8306–8319
Wang W, Zhou W, Chen D (2014) Summer high temperature extremes in Southeast China: bonding with the El Niño-Southern Oscillation and East Asian summer monsoon coupled system. J Clim 27:4122–4138
Wang W, Zhou W, Li Y, Wang X, Wang D (2015) Statistical modeling and CMIP5 simulations of hot spell changes in China. Clim Dyn 44:2859–2872
Westra S, Alexander LV, Zwiers FW (2013) Global increasing trends in annual maximum daily precipitation. J Clim 26:3904–3918
Xu Z, Sun W, Luo S, Li Y, Jiang H (2007) The variation characteristics for temperature of 3 cities of Guangdong province in the past one hundred years. J South China Normal Univ 2:137–142 (In Chinese)
Ye J, Chen Z, Gong D, Wang S (1998) Characteristics of seasonal precipitation anomalies in China for 1880–1996. Quart J Appl Meteorol 9:57–64 (In Chinese)
You Q, Kang S, Aguilar E, Pepin N, Flugel W, Yan Y, Xu Y (2010) Changes in daily climate extremes in China and their connection to the large scale atmospheric circulation during 1961–2003. Clim Dyn 36:2399–2417
Zhai PM, Zhang XB, Wan H, Pan XH (2005) Trends in total precipitation and frequency of daily precipitation extremes over China. J Clim 18:1096–1108
Zhang XB, Zwiers FW, Li GL (2004) Monte Carlo experiments on the detection of trends in extreme values. J Clim 17:1945–1952
Zhang Q, Xu CY, Becker S, Zhang ZX, Chen YD, Coulibaly M (2009) Trends and abrupt changes of precipitation maxima in the Pearl River basin, China. Atmos Sci Lett 10:132–144
Zhou W, Li CY, Chan JCL (2006) The interdecadal variations of the summer monsoon rainfall over South China. Meteorol Atmos Phys. doi:10.1007/S00703-006-018-9
Zhou W, Chan JCL, Chen W, Liang J, Pinto JG, Shao YP (2009) Synoptic-scale controls of persistent low temperature and icy weather over southern China in January 2008. Mon Weather Rev 137:3978–3991

Editorial responsibility: Bryson Bates, Wembley, WA, Australia

Submitted: October 6, 2014; Accepted: August 2, 2015
Proofs received from author(s): September 14, 2015